



1 **Geospatial Analysis of Fault–Epicerter Dynamics in Bangladesh and Adjacent Regions** 2 **Using Remote Sensing and Statistical Modeling**

3 Md. Abu Dardha Limon¹, Khandakar Hasan Mahmud¹

4 ¹Department of Geography and Environment, Jahangirnagar University, Savar, Dhaka-1342,
5 Bangladesh

6 *Correspondence to:* Md. Abu Dardha Limon (limon.48@geography-juniv.edu.bd)

7 **Abstract**

8 Bangladesh and its adjacent regions are situated at the junction of several tectonic plates and are
9 hence highly susceptible to earthquakes. This study investigates the spatial dynamics between fault
10 lines, their classifications, and earthquake epicenters in Bangladesh and its neighboring countries.
11 With a high-density population, absence of urban planning, and inter-border seismic hazards,
12 identifying the way fault types interact with seismic activity is crucial for an effective estimation
13 of the hazard in this area.

14 Landsat 8 Thermal Infrared Sensor (Band 10) satellite imagery was used for the detection of faults,
15 followed by the extraction of lineaments using PCI Geomatica and spatial analysis in ArcMap
16 10.8. Fault lines were identified as four principal types: normal, reverse, left-lateral, and right-
17 lateral, based on geometric and spatial features. Earthquake epicenter data between 1924 and 2024
18 were derived from the USGS Earthquake Catalog. Spatial autocorrelation analysis (Moran's I),
19 Kruskal-Wallis test, Dunn's test, and multinomial logistic regression were used to examine fault-
20 epicenter relationships.

21 Approximately 40,000 fault lineaments were identified. Moran's I index (0.298, $p < 0.000001$)
22 confirmed significant spatial clustering of epicenters and fault lines. Dunn's test demonstrated that
23 reverse faults significantly differ from the others in terms of proximity to epicenters. Multinomial
24 logistic regression revealed that earthquakes tend to be closer to normal ($p = 0.042$) and left-lateral
25 faults ($p = 0.016$), whereas reverse faults ($p = 0.676$) did not exhibit significant differentiation
26 based on proximity.

27 This work highlights the crucial need to incorporate fault types and epicenter spatial relationships
28 into seismic hazard models. The results offer practical insight into regional earthquake risk



29 mitigation, infrastructure design, and transboundary disaster preparedness in Bangladesh and
30 adjacent regions.

31 **Keywords:** Earthquake, Fault line, Fault line types, Epicenter, Satellite image, Statistical
32 modeling, Bangladesh

33 **1 Introduction**

34 Earthquakes are sudden ruptures in the Earth's crust or mantle caused by tectonic stress, resulting
35 in the release of seismic waves, and occur when rocks are abruptly disturbed, often along fault
36 lines where tectonic plates meet (Kanamori, 1994). They are the most disastrous of all natural
37 calamities, which damage life and property in the shortest possible time (Al-Dogom et al., 2021).
38 Earthquakes are a natural disaster that have long dynamically affected the Earth's landscape and
39 caused serious injury to living creatures, drastic changes to the living environment, and
40 catastrophic damage to the economy and infrastructure (Hossain et al., 2020). In the 20th century,
41 earthquake disasters caused casualties of close to 2 million people worldwide and claimed an
42 average of over 25,000 lives annually (Yariyan et al., 2020; Mohammadi et al., 2025). Earthquakes
43 also have the potential to cause secondary consequences such as landslides, fires, and tsunamis,
44 which pose significant risks to human life, infrastructure, and the environment (Alavi et al., 2024).

45 Bangladesh is also at risk of catastrophic earthquakes due to its position on the northeastern Indian
46 plate, which is located at the junction of three tectonic platforms: the Indian plate, the Eurasian
47 plate, and the Burmese microplate, where severe earthquakes have occurred in the past. (Morino
48 et al. 2011, 2014; Steckler et al. 2016; Biswas et al., 2018; Salman et al., 2023). In 2015, an
49 earthquake resulted in 6 deaths and over 200 injuries in the country (Biswas et al., 2016). This
50 shows the damage and also the potential for damage from earthquakes in Bangladesh. This region
51 is also seismically vulnerable due to high population density, unplanned urbanization, and non-
52 engineered construction practices (Rahman et al., 2020). Moreover, the cities of Bangladesh are
53 facing unplanned urban growth, rapid rural to urban migration, and environmental degradation,
54 which expose the urban populations to earthquake hazards. (Alam & Haque, 2022). The country
55 is affected by earthquakes originating in India and Myanmar. In order to construct a complete
56 geography of the hazard, it is necessary to consider active seismic sources from the adjacent
57 countries, particularly adjoining Bangladesh (Alam & Dominey-Howes, 2014). That is why in
58 this study, the adjacent regions of Bangladesh are included.



59 Earthquakes are processes associated with objects known as fault zones. Therefore, earthquake
60 physics is dictated to a considerable extent by fault zone properties. (Ben-Zion & Sammis, 2003).
61 Fault lines are critical features in tectonic studies, representing zones of localized motion within
62 the Earth's crust and lithosphere (Handy et al., 2007). Furthermore, fault lines significantly
63 influence earthquake behavior and attenuation. Thus, the distribution of seismic intensity and
64 damage is affected by fault mechanisms and rupture extent (Bureau, 1978).

65 Fault damage zones play a crucial role in long-term earthquake behavior, which influences
66 earthquake size variability, hypocenter locations, and seismic wave reflections. Understanding
67 fault damage zone properties could improve earthquake hazard assessments by providing insights
68 into future earthquake depths (Thakur et al., 2020). There are some methods popular for detecting
69 fault lines. Recent research revealed advanced fault detection techniques in geosciences,
70 combining geophysical, remote sensing, and computational methods (Adwan et al., 2024). Remote
71 sensing methods, including satellite imagery analysis, have proven effective in detecting both
72 active and inactive faults (Tanner et al., 2019)

73 There are mainly four fault types, e.g., reverse, normal, left-lateral, and right-lateral. (USGS,
74 2025). A significant relationship is seen between fault types and earthquake characteristics, and
75 different fault types exhibit varying TEC anomaly patterns before large earthquakes (Ulukavak et
76 al., 2022).

77 The primary objectives of the study were to identify geotectonic fault lines and fault line types in
78 Bangladesh and its adjacent regions, and to examine the spatial dynamics among fault lines, fault
79 line types, and earthquake epicenters. In this study, appropriate and up-to-date methods were used
80 to accomplish the objectives. From the study, we will determine whether there is a relationship
81 between earthquake epicenters and fault lines, and which fault type is most likely to generate an
82 earthquake in and around Bangladesh.

83 **2 Materials and methods**

84 **2.1 Study area**

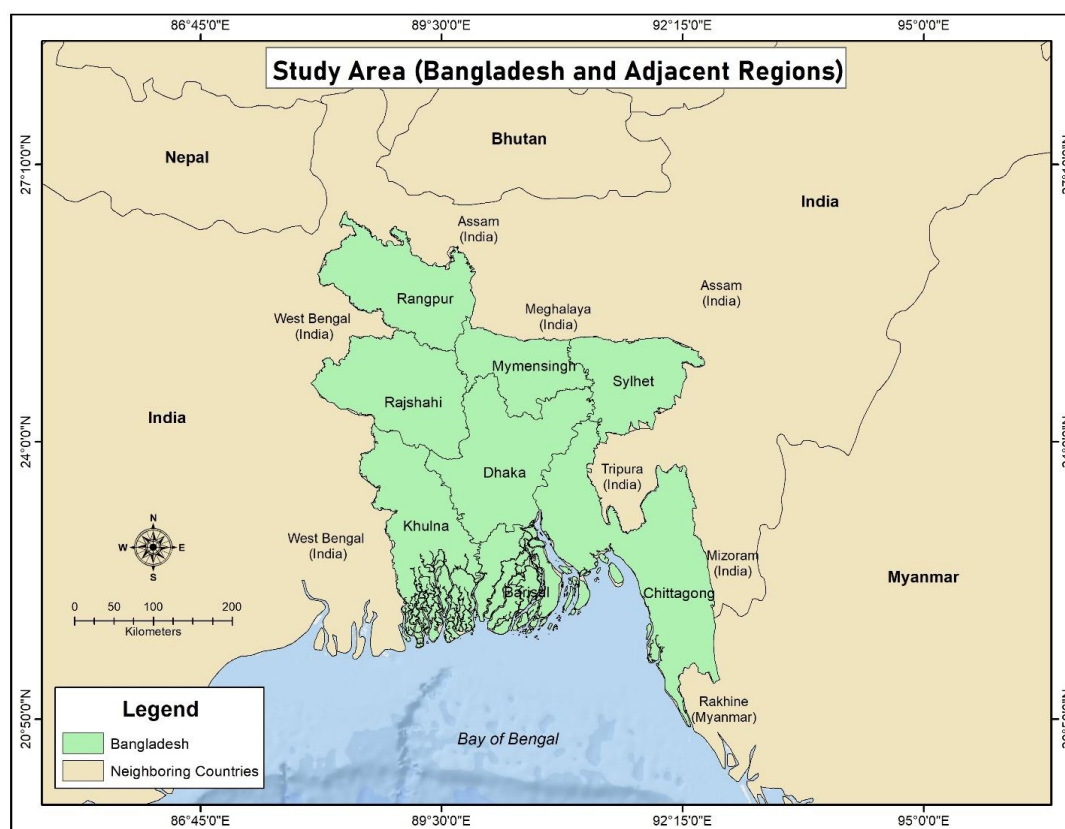
85 The study area for this study is Bangladesh and its adjacent regions, including India, Myanmar,
86 Nepal, and Bhutan, as shown in Fig. 1. This region is geologically active and forms part of the



broader Indo-Burman range and Himalayan tectonic regime, which has been recognized for its complex fault systems and seismic vulnerability (Sapkota et al., 2013; Steckler et al., 2016).

Bangladesh, which lies within latitudes $20^{\circ}34'N$ to $26^{\circ}38'N$ and longitudes $88^{\circ}01'E$ to $92^{\circ}41'E$, is bordered by the Indian states of West Bengal, Assam, Meghalaya, Tripura, and Mizoram to the west, north, and east; Rakhine State of Myanmar to the southeast; and the Bay of Bengal to the south. Internally, the study considers key administrative divisions of Bangladesh, including Dhaka, Chittagong, Sylhet, Mymensingh, Rajshahi, Rangpur, Khulna, and Barisal, which are both demographically and geographically significant (BANGLAPEDIA, 2024).

Figure 1: Study area map showing Bangladesh and its adjacent regions

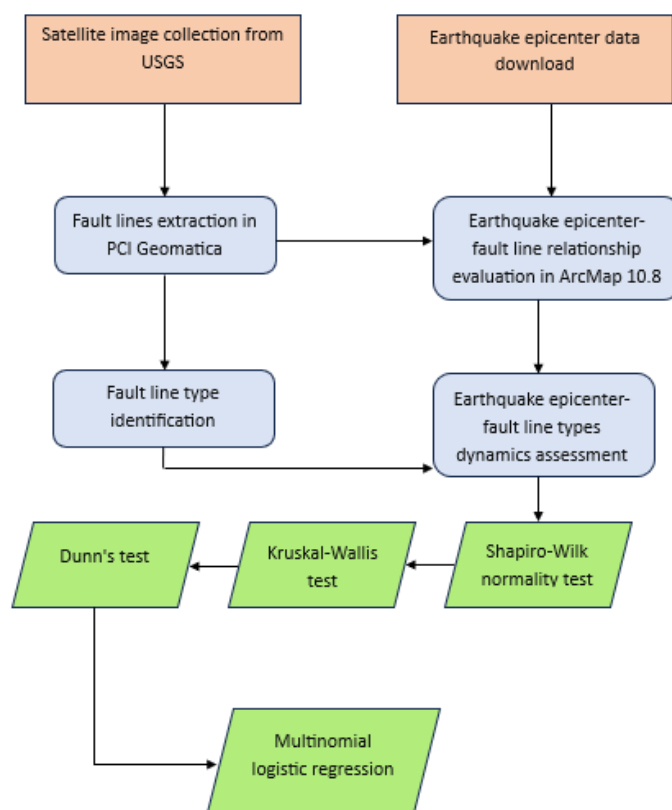


The adjacent regions of Bangladesh are prone to earthquakes as seismically active regions, such as the Himalayan Arc, the Shillong Plateau, and the Burmese Arc, are very close to this region. (Sultana et al., 2013).



100 The incorporation of adjacent Indian states and Myanmar within the study is crucial, as numerous
 101 epicentral sources and fault systems that control seismic activity in Bangladesh are either sourced
 102 or extend outside its boundaries. Transboundary seismicity and fault processes are therefore crucial
 103 for accurate risk modeling and effective regional disaster planning measures (Nath & Thingbaijam,
 104 2012).

105 Figure 2: Methodological framework of the study



106

107 2.2 Satellite image collection

108 Firstly, satellite images of Bangladesh and its adjoining areas were gathered from the USGS Earth
 109 Explorer for extracting fault lines for this region. Thermal information utilized in this study was
 110 obtained from Band 10 (10.6–11.2 μm) of the Thermal Infrared Sensor (TIRS) of Landsat 8. The



111 data were gathered from the dry season (March 2025) to minimize atmospheric interference and
112 maximize thermal surface contrast.

113 Landsat 8, a NASA-USGS collaborative mission, hosts both the Operational Land Imager (OLI)
114 and TIRS. While OLI collects multispectral reflectance, this study only considered TIRS Band 10
115 because it has greater radiometric stability and less calibration uncertainty than Band 11 (Wulder
116 et al., 2012; Roy et al., 2014). Although Band 10 possesses a native resolution of 100 meters,
117 USGS resamples it to 30 meters through cubic convolution interpolation for a more accurate and
118 higher-quality image.

119 **2.3 Fault lines extraction**

120 Systematic processing of the satellite images was conducted in PCI Geomatica software in order
121 to identify and delineate the tectonic fault lines of Bangladesh and its adjacent regions. The
122 processing workflow utilized the high-level modules of the software, i.e., the Algorithm Librarian,
123 geological analysis, and lineament extraction utilities, specifically designed for lineament
124 extraction in complex geological terrains.

125 The PCI Geomatica software's lineament extraction process is widely applied in the identification
126 of geological structures from satellite imagery. The automatic method employs the LINE module
127 in enhancing edge discontinuities and directional features. The directional convolution filters, such
128 as high-pass directional filters (3×3 , 5×5), were employed to enhance linear features with certain
129 azimuthal directions (e.g., 45° , 90° , 135°). These filters strengthen pixel intensity gradients within
130 desired directions to allow faint geological discontinuities, such as faults, joints, and fractures, to
131 be identified. Finally, once the lineaments and fault lines are extracted, they are saved as a shapefile
132 and opened with the ArcMap 10.8 software.

133 **2.4 Fault line type identification**

134 Extracted lineaments were categorized into four main fault types: normal faults, reverse faults,
135 left-lateral faults, and right-lateral faults, as they are the main fault types (USGS, 2025). The
136 classification was based on the assessment of length, curvature, intersection patterns, clustering,
137 and orientation of the faults. Earlier studies in the Indo-Burma subduction zone and the United
138 States Fault and Fold Database were used as reference templates to classify the faults (USGS,
139 2025).



140 2.5 Earthquake epicenter data acquisition

141 A 100-year (1924–2024) earthquake catalog was extracted from the USGS Earthquake Catalog, a
 142 mature and continuously revised database of historic and real-time seismicity (Hayes et al., 2019).
 143 The catalog incorporates both early instrumental and modern seismic data from seismic and
 144 geodetic networks. For accuracy in analysis, events of magnitudes ≥ 3.0 only were extracted, as
 145 lower-magnitude micro-seismic events are often underreported in older records and provide
 146 minimal information on structural damage potential or regional stress distribution. The raw dataset
 147 was then exported in CSV format and opened in ArcMap 10.8 software, where it was converted
 148 into a geodatabase feature layer through the Add Data and Add XY Data tools.

149 Geospatial filtering was applied using a custom boundary polygon that covered tectonically
 150 relevant regions, including Bangladesh, West Bengal, parts of Nepal and Bhutan, the Bay of
 151 Bengal, northeast India (Assam, Meghalaya, Mizoram, and Tripura), and western Myanmar. There
 152 were 1541 earthquake epicenter data filtered from the process for the specific region.

153 2.6 Earthquake epicenter and fault line proximity analysis

154 To statistically investigate whether earthquake epicenters are correlated with fault lines or not, a
 155 proximity-based spatial analysis was performed using ArcMap 10.8 software. Specifically, the
 156 "Near" tool within the ArcToolbox > Analysis Tools > Proximity module was used to calculate the
 157 shortest Euclidean distance from the epicenter of each earthquake to its closest fault line. The
 158 distance from an earthquake epicenter to the closest fault line is then saved to the geodatabase of
 159 the earthquake epicenter shapefile.

160 After this, the geodatabase is converted into Excel data, which is based on fault line types and the
 161 distance from the nearest fault line to the earthquake epicenter. The Euclidean distance formula is,

$$162 \text{ Distance}_{ij} = \sqrt{(X_i - X_j)^2 + (Y_i - Y_j)^2}$$

163 Here,

- 164 • (X_i, Y_i) : coordinates of feature i in the input layer.
- 165 • (X_j, Y_j) : coordinates of feature j in the near layer.

166 2.7 Spatial dynamics between fault lines and earthquakes



167 After calculation of the shortest distance of earthquake epicenters to the nearest fault lines, spatial
 168 autocorrelation (Moran's I) was conducted in ArcMap 10.8 software. Moran's I, a global statistic,
 169 was utilized to determine the extent of spatial autocorrelation within the dataset through the
 170 provided variables. It attempts to test whether the pattern with which a variable is spread
 171 throughout space is significantly different from a random spatial process. Moran's I is a standard
 172 spatial autocorrelation measure where positive results would indicate clustering of similar values
 173 and negative results show dispersion (Zhang & Lin, 2007). The result of Moran's I shows whether
 174 there exists spatial dependency in a dataset or not.

175 Moran's I mathematical formula:

$$176 \quad I = \frac{n}{W} \cdot \frac{\sum_{i=1}^n \sum_{j=1}^n w_{ij} (x_i - \bar{x})(x_j - \bar{x})}{\sum_{i=1}^n (x_i - \bar{x})^2} \quad (\text{Moran, 1950})$$

177 Where:

178• I: Moran's I statistic

179• n: Total number of spatial units

180• x_i, x_j : Attribute values for features i and j

181• \bar{x} : Mean of the attribute values

182• w_{ij} : Spatial weight between features i and j

183• W: Sum of all spatial weights

184 **2.8 Fault line types and earthquake epicenter relationship assessment**

185 **2.8.1 Normality check and hypothesis test**

186 To investigate the relationship between fault line types and their nearest distance from earthquake
 187 epicenters, it was crucial to ascertain whether the dataset was normally distributed. This would
 188 establish whether the data required a parametric or nonparametric statistical analysis.

189 In this study, the Shapiro-Wilk normality test was used to determine the distribution of the data.
 190 The test has long been established as being sensitive in detecting non-normality and is widely
 191 recognized as an effective tool for normality checking in samples. The analysis was conducted



192 using the R programming language (version 4.3.2), applying the Shapiro-Wilk test () function from
 193 R's base statistical package.

194 The Shapiro-Wilk test gives a W statistic, and values considerably less than 1.0 indicate non-
 195 normality. The null hypothesis assumes that the data follow a normal distribution; thus, small p-
 196 values (<0.05) lead to null hypothesis rejection, indicating non-normality (Shapiro, 2019). In this
 197 study, the Shapiro-Wilk test output is $W = 0.61438$, $p\text{-value} = 2.2e-16$. The 0.61438 value of W is
 198 considerably less than 1, and the p-value is much lower than the conventional α level of 0.05,
 199 suggesting strong evidence against the null hypothesis (Fisher, 1925).

200 It can, therefore, be said that the aforesaid variable is not normally distributed. This finding
 201 necessitated the use of nonparametric statistical methods in future analysis of the dataset (Nahm,
 202 2016). Therefore, the Kruskal-Wallis rank sum test was used to examine the spatial correlation of
 203 epicentral proximity with fault line classifications. The Kruskal-Wallis test is a nonparametric
 204 statistical method used in calculating differences between three or more independent groups based
 205 on one non-normally distributed continuous variable. (Kruskal & Wallis, 1952).

206 The result of the Kruskal-Wallis rank sum test for the dataset is $\chi^2 = 22.10$, $p\text{-value} = 6.216 \times 10^{-5}$.
 207 The chi-squared statistic ($\chi^2 = 22.10$) on 3 degrees of freedom is used to test for a statistically
 208 significant difference between the distribution of shortest epicentral distances in the four types of
 209 faults. The p-value (<0.0001) is significantly smaller than the significance level ($\alpha = 0.05$), leading
 210 to the rejection of the null hypothesis that all group medians are identical.

211 This result means that at least one fault type category has a different pattern of epicentral distance
 212 from the other fault categories. However, the Kruskal-Wallis rank sum test does not specify which
 213 groups are different, so a post-hoc pairwise comparison is required. For this purpose, Dunn's test
 214 with a Bonferroni correction was then applied. Dunn's test is a nonparametric multiple comparison
 215 procedure for pairwise comparisons after finding a significant Kruskal-Wallis test (Dinno, 2015).

216 **2.8.2 Multinomial logistic regression**

217 Multinomial logistic regression was used to determine which fault type is more likely to generate
 218 an earthquake around it. Here, the dependent variables were the fault types (reverse, right-lateral,
 219 left-lateral, and normal), and the independent variables were the distance from the earthquake
 220 epicenter to the nearest fault line. This statistical technique is suitable for describing relationships



221 where the dependent variable has more than two categories and the independent variables are
222 continuous or categorical. The method estimates various binary logistic regression models for each
223 category of the dependent variable relative to a reference category (Aziz et al., 2016).

224 In this analysis, the reference category was the right-lateral fault lines, and the model estimates the
225 log-odds of membership in each of the remaining categories relative to the reference category
226 based on changes in the predictor variable. The software used to analyze the dataset was IBM
227 SPSS Statistics 21.

228 **3 Results**

229 **3.1 Fault lines in Bangladesh and its adjacent regions**

230 Figure 3: Fault lines in Bangladesh and its adjacent regions

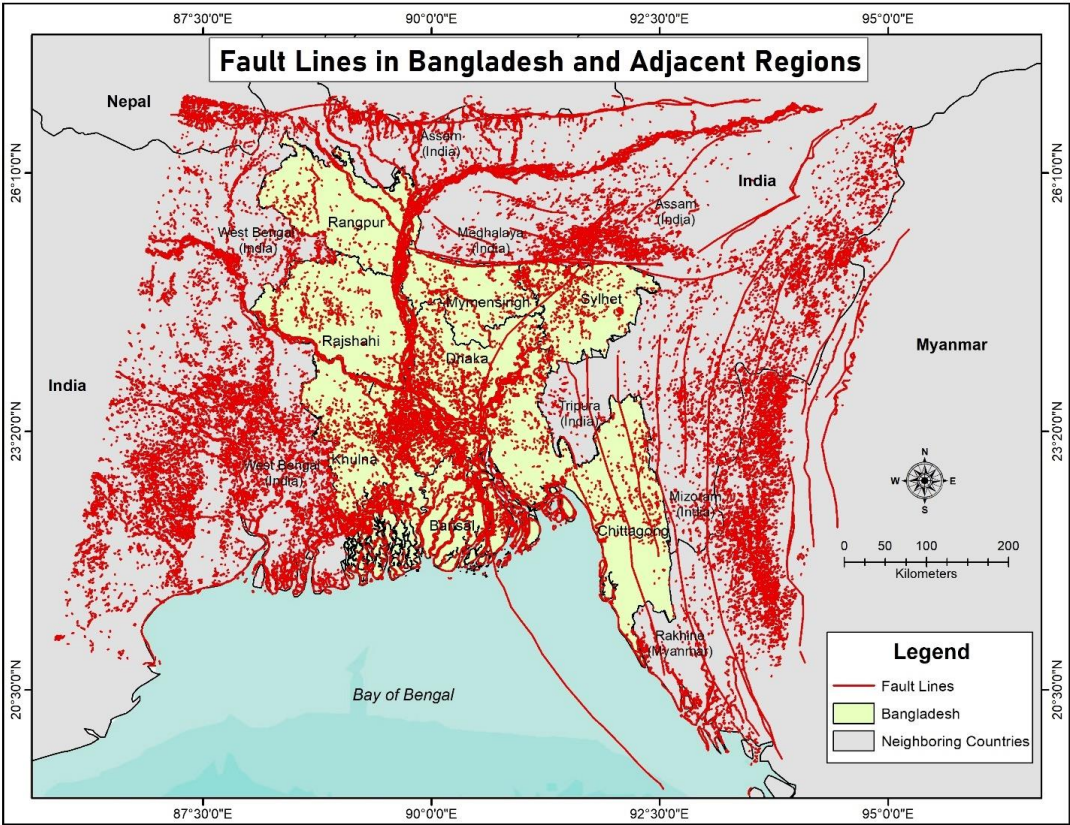




Figure 3 displays a tectonic context of Bangladesh and its adjacent regions comprising approximately 40,000 mapped fault lines and lineaments derived from advanced remote sensing and geospatial analysis. Red linear items represent active faults and seismogenic lineaments.

3.2 Fault line types in Bangladesh and its adjacent regions

Figure 4: Fault line types in Bangladesh and its adjacent regions

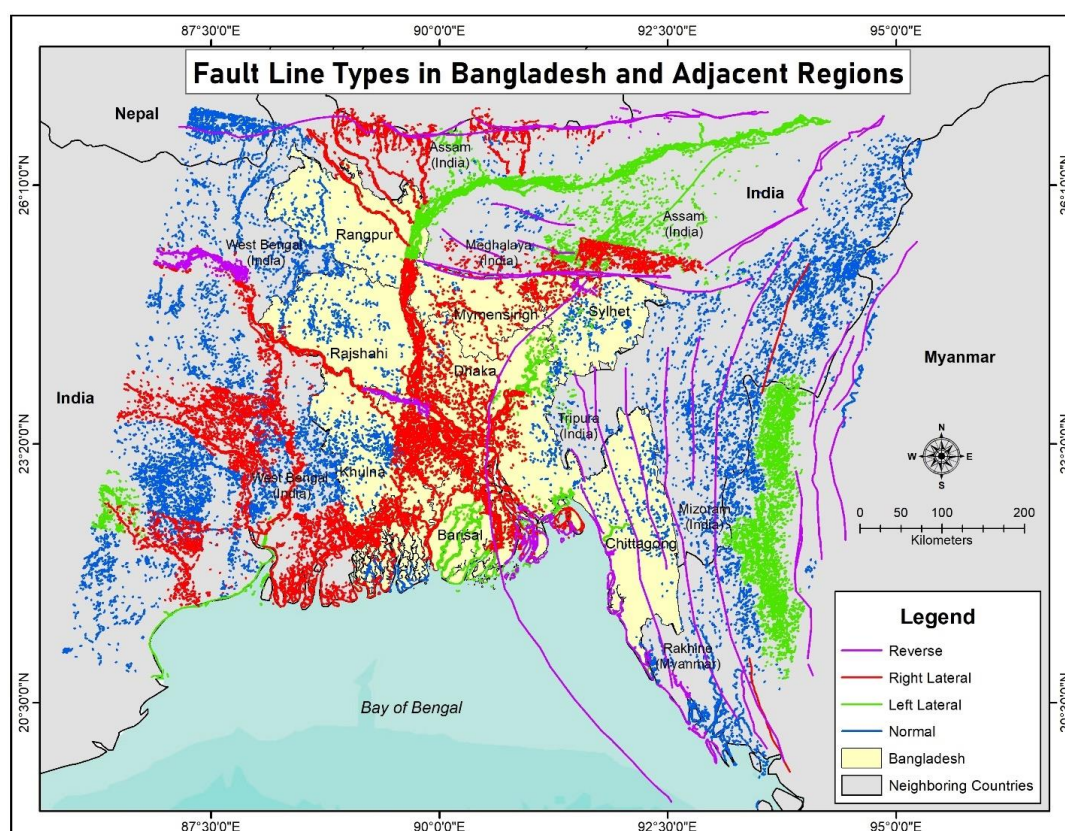
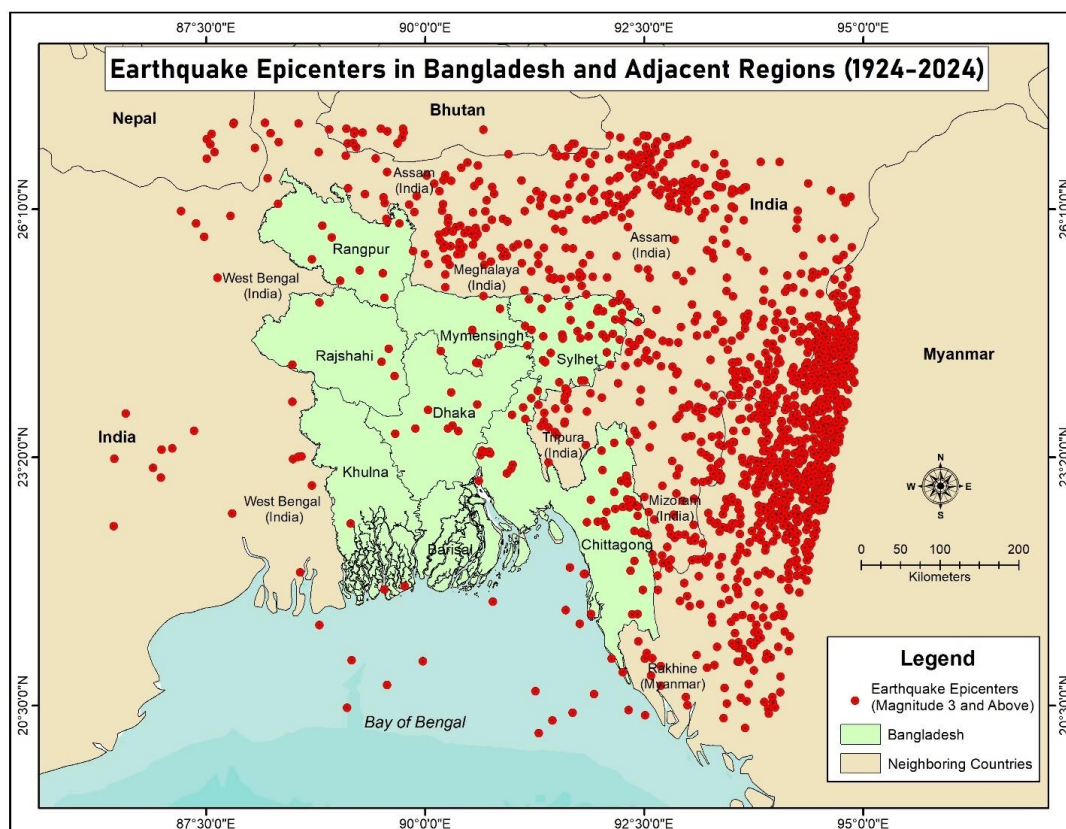


Figure 4 illustrates a more accurate spatial classification of tectonic structures in Bangladesh and the adjacent regions, delineating four major types of faults: reverse, right-lateral, left-lateral, and normal faults.

3.3 Earthquake epicenters in Bangladesh and its adjacent regions (1924-2024)

Figure 5: Earthquake epicenters in Bangladesh and its adjacent regions (1924-2024)

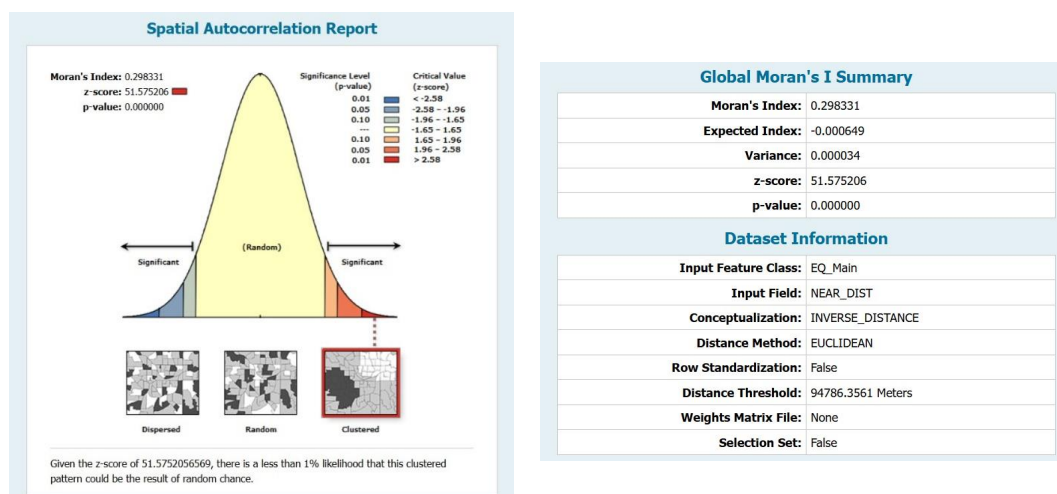


243

244 Figure 5 shows the epicentral spatial pattern of earthquake events (magnitudes ≥ 3.0) in
 245 Bangladesh and adjacent areas over the last one hundred years (1924–2024) based on seismic
 246 information offered by the USGS Earthquake Catalog. The red dots represent single earthquake
 247 events and indicate regional patterns of seismicity.

248 3.4 Earthquake epicenter and fault line relationship assessment

249 Figure 6: Spatial autocorrelation report between earthquake epicenters and fault lines



250

251 The Moran's Index report shows the spatial autocorrelation between earthquake epicenters and
 252 fault lines, highlighting the degree to which their distribution exhibits a non-random spatial pattern.

253 3.5 Earthquake epicenter and fault line type relationship assessment

254 As the Kruskal-Wallis test showed significant differences, Dunn's test will help to identify which
 255 specific fault type pairs differ significantly in terms of their distance from epicenters. Interpretation
 256 of Dunn's test result as follows,

257 Table 1: Interpretation of the Dunn's test of fault line pairs with nearest distance to epicenters

Comparison	Mean rank difference	p-value	significance
Normal vs Left-lateral	17.09	1.00000	Not significant
Reverse vs Left-lateral	259.64	0.00021	Significant
Right-lateral vs Left-lateral	-92.00	0.40750	Not significant
Reverse vs Normal	242.55	0.00071	Significant
Right-lateral vs Normal	-109.09	0.19063	Not significant



Right-lateral vs Reverse	-351.64	0.00003	Significant
-----------------------------	---------	---------	-------------

3.5.1 Assessment of the influence of specific fault lines in earthquake epicenters

A multinomial logistic regression was conducted to assess the influence of distance from earthquake epicenters on the likelihood of different fault types. The right-lateral faults were used as the reference category.

Table 2: Multinomial logistic regression of fault line types and their nearest distances from earthquake epicenters

Parameter Estimates									
Nearest fault distance		B	Std. Error	Wald	df	Significance	Exp(B)	95% Confidence Interval for Exp(B)	
								Lower Bound	Upper Bound
Left-Lateral	Intercept	2.321	.137	288.871	1	.000			
	Near-Distance	-2.829	1.177	5.780	1	.016	.059	.006	.593
Normal	Intercept	2.151	.137	245.719	1	.000			
	Near-Distance	-2.364	1.164	4.124	1	.042	.094	.010	.921
Reverse	Intercept	-.520	.201	6.648	1	.010			
	Near-Distance	.571	1.367	.174	1	.676	1.769	.121	25.773
a. The reference category is: Right-lateral.									

The multinomial logistic regression model captured valuable information on spatial relationships between the locations of earthquake epicenters and fault types. Using fault types as the dependent variable and the distance from an epicenter to the nearest fault line (Near-Distance) as the



independent variable, the model estimated the probability of the occurrence of earthquakes near different types of faults relative to right-lateral faults (the reference category).

4 Discussion

4.1 Fault lines in Bangladesh and its adjacent regions

In Fig. 3, active faults have long, continuous, and sharply defined geometries. They are most prominent along the eastern and northeastern boundary of Bangladesh, including zones around Myanmar, the Tripura-Mizoram fold belt, and the Dauki Fault zone along the Shillong Plateau in Meghalaya. These zones have been traditionally associated with great-magnitude seismic activities, including the 1897 Great Assam Earthquake ($M_w \sim 8.0$) (Morino et al., 2011)

In contrast, lineaments, which have linear orientation, do not necessarily all overlie currently active faults, but tend to define areas of tectonic weakness. They are highest in central and southern Bangladesh, the Sylhet trough, and West Bengal, India. Lineaments play a crucial role in shaping the region's morphology. Although lineaments may lack direct evidence for surface rupture, their alignment along with known stress orientations and seismic clusters suggests that the majority can be reactivated during subsequent seismic cycles. The significance of lineaments and faults in understanding seismic activity has gained emphasis through recent research. Lamontagne et al. (2020) mapped lineaments and faults in seismically active regions of Quebec and Ontario and provided a comprehensive overview of brittle structures.

4.2 Fault line types in Bangladesh and its adjacent regions

In Fig. 4, right-lateral faults are present with dense concentration in central and southern Bangladesh, from Dhaka to Khulna and the Meghna Delta. Right-lateral faulting is associated with horizontal shear and rotation of the blocks in a variety of tectonic regimes (Ron et al., 1984). The same faulting mechanisms were identified in the Sundarbans region, indicating active shearing on the delta front. The left-lateral faults are well-structured along the Meghalaya Plateau, Barisal division, and west of Myanmar near Mizoram. The left-lateral faults are anticipated in oblique convergent regimes, where the crustal shortening and lateral translation are co-temporal (Morino et al., 2011).



294 Normal faults occur dominantly in the Rajshahi division, West Bengal, and northeast India. Normal
 295 faults are a widespread feature of extensional tectonic regimes, with downward movement of the
 296 hanging wall above the footwall (Jackson & McKenzie, 1983).

297 Reverse faults are focused in the Chittagong Hill Tracts, southern Mizoram, Meghalaya to the east
 298 of Sylhet, and Myanmar's Rakhine state. Reverse faults are a result of compressional stress,
 299 characteristic of convergent tectonic boundaries. This style is the one that best fits the forecasted
 300 tectonic response of the Indo-Burman subduction system, where the Indian Plate is being
 301 subducted under the Burma Plate (Steckler et al., 2008). The area has experience with megathrust
 302 earthquakes, e.g., the 1762 Arakan earthquake (Wang et al., 2014).

303 **4.3 Earthquake epicenters in Bangladesh and its adjacent regions (1924-2024)**

304 The distribution of earthquake epicenters in Fig. 5 displays distinct spatial clustering, with
 305 comparatively high concentrations in the Indo-Burma subduction zone, the Tripura-Mizoram fold
 306 belt, and northeastern India, particularly in Assam and Meghalaya. The clusters coincide with main
 307 active fault systems and known tectonic boundaries, for example, the Dauki Fault in Meghalaya,
 308 the Chittagong-Tripura-Mizoram thrust front. This is consistent with previous observations that
 309 the region has experienced deep oblique convergence of the Indian Plate and the Burma
 310 Microplate, resulting in an elevated level of moderate-to-large seismicity (Steckler et al., 2008;
 311 Wang et al., 2014). Seismicity in Bangladesh is most vigorous in the Chittagong Hill Tracts and
 312 Sylhet areas, where seismic hazard potential is increased by proximity to compressional and
 313 transpressional fault systems.

314 **4.4 Earthquake epicenter and fault line relationship assessment**

315 From Fig. 6, it can be seen that the spatial autocorrelation analysis produced Moran's Index of
 316 0.298, indicating moderate and statistically significant positive spatial autocorrelation. This would
 317 suggest that earthquake occurrences with similar fault proximities are more likely to cluster
 318 spatially than they would be randomly distributed. The z-score of 51.575 and p-value of <0.000001
 319 unequivocally support the assertion that such clustering is highly improbable by random chance.
 320 These are considerably above 99% critical levels of a typical significance curve with data
 321 distribution in the clustered tail of the curve. The trend shows that seismic activity is not randomly



distributed over the area but rather tends to accumulate in regions where faults are in close alignment or tectonically active.

4.5 Earthquake epicenter and fault line type relationship assessment

Table 1 illustrates that reverse faults have appreciably different (larger) distances from left-lateral, normal, and right-lateral faults, as the p-value for reverse faults is appreciably lower than 0.05, grouping with the other three faults. Right-lateral, normal, and left-lateral faults are not appreciably different from each other, as no statistically significant difference was noted among these faults. Therefore, reverse fault types differ from the remaining types of faults in terms of distance from earthquake epicenters in this study.

4.5.1 Assessment of the influence of specific fault lines in earthquake epicenters

Table 2 shows that the distance to normal and left-lateral faults exerts a significant effect on earthquake occurrence probability. To be specific, distance to left-lateral faults was strongly negatively correlated ($B = -2.829$, $p = 0.016$), i.e., earthquakes have an extremely high chance of occurring near left-lateral faults compared to right-lateral faults. Similarly, for normal faults, the distance parameter was also negatively significant ($B = -2.364$, $p = 0.042$), revealing a higher likelihood that earthquakes would occur close to normal faults as well. These observations are evidence of spatial clustering of earthquake activity in the vicinity of these two fault types, and they conclude that their structural and tectonic character can be more seismically favorable in the region. Conversely, there was a non-significant statistical relationship between distance and reverse faults ($B = 0.571$, $p = 0.676$), and the wide confidence range of the odds ratio ($\text{Exp}(B) = 1.769$, 95% Confidence Interval: 0.121–25.773) suggests very high uncertainty in the relationship. This lack of relevance can result in a statement that reverse faults have decreased seismic productivity compared to left-lateral and normal faults.

The findings validate the usefulness of integrating statistical modeling, remote sensing, and geospatial data for exposing small fault-epicenter patterns. By identifying fault types more likely to trigger nearby earthquakes, the model helps to include a more realistic representation of seismic hazard distribution. The left-lateral and normal faults had the highest correlations with earthquake proximity, suggesting that the faults are likely to be more active or structurally better developed, in concordance with regional directions of stress. This approach enables probabilistic fault



351 behavior modeling in addition to deterministic fault mapping and provides a valuable tool for
352 seismic risk area ranking.

353 **5 Conclusions**

354 This study conducts a rigorous geospatial and statistical analysis of fault lines, fault line types, and
355 their spatial relationship with earthquake epicenters within Bangladesh and the adjacent regions.
356 Using advanced remote sensing techniques, thermal infrared satellite imagery, and spatial
357 characteristics of faults, the study was able to identify and classify fault lines into four broad
358 categories: reverse, normal, left-lateral, and right-lateral, highlighting their geotectonic
359 significance.

360 Through spatial autocorrelation analysis, the study demonstrated that earthquake epicenters are not
361 randomly distributed but rather cluster near specific fault systems. Nonparametric statistical testing
362 (Dunn's test, Kruskal-Wallis) verified that reverse faults differ significantly from the other fault
363 types in epicentral proximity, establishing their distinct seismic behavior. Multinomial logistic
364 regression also verified that earthquakes are more likely to occur at distances near normal faults
365 and left-lateral faults in a detailed fault line system in and around Bangladesh.

366 These findings emphasize the fundamental requirement for incorporating fault type and their
367 proximity to earthquake epicenters into regional earthquake hazard models. The methodology and
368 results provide useful suggestions for disaster planning, infrastructure construction, and seismic
369 hazard mitigation in Bangladesh and neighboring countries. Moreover, cross-border seismic
370 source consideration confirms the importance of regional collaboration in sustainable earthquake
371 resilience planning for Bangladesh.

372 **Data availability**

373 The data supporting this study are available from the corresponding author upon reasonable
374 request.

375 **Author contribution**

376 MADL: conceptualization, data curation, methodology, supervision, software, formal analysis,
377 validation, visualization, and writing (original draft preparation as well as review and editing).
378 KHM: conceptualization, supervision, software, visualization, writing (review and editing).



379 **Competing interests**

380 The contact author has declared that none of the authors has any competing interests.

381 **Disclaimer**

382 Copernicus Publications remains neutral with regard to jurisdictional claims made in the text,
383 published maps, institutional affiliations, or any other geographical representation in this paper.
384 While Copernicus Publications makes every effort to include appropriate place names, the final
385 responsibility lies with the authors.

386 **References**

- 387 Adwan, A., Maillot, B., Souloumiac, P., and Barnes, C.: Fault detection methods for 2D and
388 3D geomechanical numerical models. *Int. J. Numer. Anal. Methods Geomech.*, 48, 607–625,
389 <https://doi.org/10.1002/nag.3652>, 2024.
- 390 Alam, E., and Dominey-Howes, D.: An analysis of the AD1762 earthquake and tsunami in SE
391 Bangladesh, *Nat Hazards* 70, 903–933. Kluwer Academic Publishers.
392 <https://doi.org/10.1007/s11069-013-0841-5>, 2014.
- 393 Alam, M. S., and Haque, S. M.: Multi-dimensional earthquake vulnerability assessment of
394 residential neighborhoods of Mymensingh City, Bangladesh: A spatial multi-criteria analysis-
395 based approach. *J. Urban Manag.*, 11, 37–58, <https://doi.org/10.1016/j.jum.2021.09.001>, 2022.
- 396 Alavi, S. H., Bahrami, A., Mashayekhi, M., and Zolfaghari, M.: Optimizing Interpolation
397 Methods and Point Distances for Accurate Earthquake Hazard Mapping, *Buildings*, 14, 1–25,
398 <https://doi.org/10.3390/buildings14061823>, 2024.
- 399 Al-Dogom, D., Al-Ruzouq, R., Kalantar, B., Schuckman, K., Al-Mansoori, S., Mukherjee, S.,
400 Al-Ahmad, H., and Ueda, N.: Geospatial Multicriteria Analysis for Earthquake Risk
401 Assessment: Case Study of Fujairah City in the UAE, *J. Sens.*, 2021, 1–25,
402 <https://doi.org/10.1155/2021/6638316>, 2021.
- 403 Aziz, N. A. A., Ali, Z., Nor, N. M., Baharum, A., and Omar, M. Modeling Multinomial Logistic
404 Regression on Characteristics of Smokers after the Smoke-Free Campaign in the Area of
405 Melaka. *AIP Conf. Proc.*, 1750, <https://doi.org/10.1063/1.4954625>, 2016.



- 406 Bangladesh, BANGLAPEDIA: National Encyclopedia of Bangladesh,
 407 <https://en.banglapedia.org/index.php/Bangladesh>, 2024.
- 408 Ben-Zion, Y., and Sammis, C. G.: Characterization of Fault Zones, *Pure Appl. Geophys.*, 160,
 409 677–715, 2003.
- 410 Bilham, R.: Himalayan earthquakes: a review of historical seismicity and early 21st-century
 411 slip potential, *Geol. Soc. Spec. Publ.*, 483, 423–482, Geological Society of London.
 412 <https://doi.org/10.1144/SP483.16>, 2019.
- 413 Biswas, A., Mashreky, S. R., Dalal, K., and Deave, T.: Response to an Earthquake in
 414 Bangladesh: Experiences and Lesson Learnt, *Open J. Earthq. Res.*, 5, 1–6,
 415 <https://doi.org/10.4236/ojer.2016.51001>, 2016.
- 416 Biswas, R. N., Islam, M. N., and Islam, M. N.: Modeling on management strategies for spatial
 417 assessment of earthquake disaster vulnerability in Bangladesh, *Model. Earth Syst. Environ.*, 4,
 418 1377–1401, <https://doi.org/10.1007/s40808-018-0507-0>, 2018.
- 419 Dinno, A.: Nonparametric pairwise multiple comparisons in independent groups using Dunn’s
 420 test, *Stata J.*, 15, 292–300, 2015.
- 421 Faults, U.S. Geological Survey. <https://www.usgs.gov/programs/earthquake-hazards/faults>,
 422 2025.
- 423 Fisher, R. A.: Statistical methods for research workers, Edinburgh, Scotland, Oliver and Boyd,
 424 1925.
- 425 Handy, M.R., Hirth, G., & Hovius, N.: Tectonic Faults: Agents of Change on a Dynamic Earth,
 426 <https://doi.org/10.7551/mitpress/6703.001.0001>, 2007.
- 427 Hayes, G. P., Earle, P. S., Benz, H. M., Wald, D. J., and Yeck, W. L.: National Earthquake
 428 Information Center Strategic Plan, 2019–23, US Geological Survey Circular, 1457, 1–20.
 429 <https://doi.org/10.3133/cir1457>, 2019.
- 430 Hossain, M. S., Rahaman, M. M., and Khan, R. A.: Active Seismic Structures, Energy
 431 Infrastructures, and Earthquake Disaster Response Strategy-Bangladesh Perspective. *Int.*
 432 *Energy J.*, 20, 509–522, 2020.



- 433 Jackson, J., and McKenzie, D.: The geometrical evolution of normal fault systems, *J. Struct.*
 434 *Geol.*, 5, 471–482, 1983.
- 435 Kanamori, H.: MECHANICS OF EARTHQUAKES, *Annu. Rev. Earth Planet. Sci.*, 22, 207–
 436 237, 1994.
- 437 Kruskal, W. H., and Wallis, W. A.: Use of ranks in one-criterion variance analysis, *J. Am. Stat.*
 438 *Assoc.*, 47, 583–621, 1952.
- 439 Lamontagne, M., Brouillette, P., Gregoire, S., Bédard, M.P., and Bleeker, W.: Faults and
 440 lineaments of the Western Quebec Seismic Zone, Quebec and Ontario,
 441 <https://doi.org/10.4095/321900>, 2020.
- 442 Mohammadi, S., Balouei, F., Amini, S., and Rabiei-Dastjerdi, H.: Beyond the richter scale: a
 443 fuzzy inference system approach for measuring objective earthquake risk. *Nat. Hazards*, 121,
 444 245–268, <https://doi.org/10.1007/s11069-024-06786-9>, 2025.
- 445 Moran, P. A. P.: Notes on Continuous Stochastic Phenomena, *Biometrika*, 37, 17–23,
 446 <https://doi.org/10.2307/2332142>, 1950.
- 447 Morino, M., Kamal, A. S. M. M., Akhter, S. H., Rahman, M. Z., Ali, R. M. E., Talukder, A.,
 448 Khan, M. M. H., Matsuo, J., and Kaneko, F.: A paleo-seismological study of the Dauki fault at
 449 Jafalong, Sylhet, Bangladesh: Historical seismic events and an attempted rupture segmentation
 450 model, *J. Asian Earth Sci.*, 91, 218–226. <https://doi.org/10.1016/j.jseaes.2014.06.002>, 2014.
- 451 Morino, M., Maksud, A. S. M. M., Muslim, D., Ali, R. M. E., Kamal, M. A., Rahman, M.Z.,
 452 and Kaneko, F.: Seismic event of the Dauki Fault in 16th century confirmed by trench
 453 investigation at Gabrakhari Village, Haluaghat, Mymensingh, Bangladesh, *J. Asian Earth Sci.*,
 454 42, 492–498, <https://doi.org/10.1016/j.jseaes.2011.05.002>, 2011.
- 455 Nahm, F. S.: Nonparametric statistical tests for the continuous data: The basic concept and the
 456 practical use, *Korean J. Anesthesiol.*, 69, 8–14, <https://doi.org/10.4097/kjae.2016.69.1.8>, 2016.
- 457 Nath, S. K., and Thingbaijam, K. K. S.: Probabilistic seismic hazard assessment of India,
 458 *Seismol. Res. Lett.*, 83, 135–149, <https://doi.org/10.1785/gssrl.83.1.135>, 2012.



- 459 Rahman, M. Z., Siddiqua, S., and Kamal, A. S. M. M.: Seismic source modeling and
 460 probabilistic seismic hazard analysis for Bangladesh, *Nat. Hazards*, 103, 2489–2532,
 461 <https://doi.org/10.1007/s11069-020-04094-6>, 2020.
- 462 Ron, H., Freund, R., Garfunkel, Z., and Nur, A.: Block rotation by strike-slip faulting:
 463 structural and paleomagnetic evidence, *J. Geophys. Res.*, 89, 6256–6270,
 464 <https://doi.org/10.1029/JB089iB07p06256>, 1984.
- 465 Roy, D. P., Wulder, M. A., Loveland, T. R., C.E., W., Allen, R. G., Anderson, M. C., Helder,
 466 D., Irons, J. R., Johnson, D. M., Kennedy, R., Scambos, T. A., Schaaf, C. B., Schott, J. R.,
 467 Sheng, Y., Vermote, E. F., Belward, A. S., Bindaschadler, R., Cohen, W. B., Gao, F., ... Zhu, Z.:
 468 Landsat-8: Science and product vision for terrestrial global change research, *Remote Sens.*
 469 *Environ.*, 145, 154–172, <https://doi.org/10.1016/j.rse.2014.02.001>, 2014
- 470 Salman, M. A., Nomaan, M. S. S., and Saha, A.: An updated earthquake catalog for
 471 Bangladesh: an attempt at a seismic risk evaluation, *Geology Geophys. Environ.*, 49, 37–51,
 472 <https://doi.org/10.7494/geol.2023.49.1.37>, 2023.
- 473 Sapkota, S. N., Bollinger, L., Klinger, Y., Tapponnier, P., Gaudemer, Y., and Tiwari, D.: Primary
 474 surface ruptures of the great Himalayan earthquakes in 1934 and 1255, *Nat. Geosci.*, 6, 71–76,
 475 <https://doi.org/10.1038/ngeo1669>, 2013.
- 476 Shapiro, S.S.: Goodness-of-Fit Tests. The Exponential Distribution, 2019.
- 477 Steckler, M. S., Akhter, S. H., and Seeber, L.: Collision of the Ganges-Brahmaputra Delta with
 478 the Burma Arc: Implications for earthquake hazard. *Earth Planet. Sci. Lett.*, 273, 367–378,
 479 <https://doi.org/10.1016/j.epsl.2008.07.009>, 2008.
- 480 Steckler, M. S., Mondal, D. R., Akhter, S. H., Seeber, L., Feng, L., Gale, J., Hill, E. M., and
 481 Howe, M.: Locked and loading megathrust linked to active subduction beneath the Indo-
 482 Burman Ranges, *Nat. Geosci.*, 9, 615–618, <https://doi.org/10.1038/ngeo2760>, 2016.
- 483 Sultana, S., Rahman, U., and Saika, U.: EARTHQUAKE, CAUSE SUSCEPTIBILITY AND
 484 RISK MITIGATION IN BANGLADESH, *ARN J. Earth Sci.*, 2, 70–80.



- 485 Tanner, D. C., Buness, H., Igel, J., Günther, T., Gabriel, G., Skiba, P., Plenefisch, T.,
 486 Gester mann, N., and Walter, T. R.: Fault detection. *Understanding Faults: Detecting, Dating,*
 487 *and Modeling*, 81–146, Elsevier, <https://doi.org/10.1016/B978-0-12-815985-9.00003-5>, 2019.
- 488 Thakur, P., Huang, Y., and Kaneko, Y.: Effect of fault damage zones on long-term earthquake
 489 behavior on mature strike-slip faults. *JGR Solid Earth*,
 490 <http://dx.doi.org/10.31223/osf.io/bn7qg>, 2020.
- 491 Ulukavak, M., Yalçinkaya, M., Kayıkçı, E. T., Öztürk, S., Kandemir, R., and Karşı, H.:
 492 Investigation of the Relationship among Fault Types, Focal Depths, and Ionospheric TEC
 493 Anomalies before Large Earthquakes between 2000 and 2020. *J. Surv. Eng.*, 148,
 494 [https://doi.org/10.1061/\(asce\)su.1943-5428.0000395](https://doi.org/10.1061/(asce)su.1943-5428.0000395), 2022.
- 495 Wang, Y., Sieh, K., Tun, S. T., Lai, K. Y., and Myint, T.: Active tectonics and earthquake
 496 potential of the Myanmar region. *J. Geophys. Res. Solid Earth.*, 119, 3767–3822,
 497 <https://doi.org/10.1002/2013JB010762>, 2014.
- 498 What is a fault, and what are the different types?: U.S. Geological Survey.
 499 <https://www.usgs.gov/faqs/what-a-fault-and-what-are-different-types>, 2025.
- 500 Wulder, M. A., Masek, J. G., Cohen, W. B., Loveland, T. R., and Woodcock, C. E.: Opening
 501 the archive: How free data has enabled the science and monitoring promise of Landsat,
 502 *Remote Sens. Environ.*, 122, 2–10, <https://doi.org/10.1016/j.rse.2012.01.010>, 2012.
- 503 Yariyan, P., Zabihi, H., Wolf, I. D., Karami, M., and Amiriyan, S.: Earthquake risk assessment
 504 using an integrated Fuzzy Analytic Hierarchy Process with Artificial Neural Networks based
 505 on GIS: A case study of Sanandaj in Iran, *Int. J. Disaster Risk Reduct.*, 50,
 506 <https://doi.org/10.1016/j.ijdr.2020.101705>, 2020.
- 507 Zhang, T., and Lin, G.: A decomposition of Moran’s I for clustering detection,
 508 *Comput. Stat. Data Anal.*, 51, 6123–6137, <https://doi.org/10.1016/j.csda.2006.12.032>, 2007.